



*Research article*

## **Observer-based finite-time adaptive fuzzy back-stepping control for MIMO coupled nonlinear systems**

**Chao Wang<sup>1</sup>, Cheng Zhang<sup>1,\*</sup>, Dan He<sup>2</sup>, Jianliang Xiao<sup>1</sup> and Liyan Liu<sup>1</sup>**

<sup>1</sup> School of Computer Engineering, City Institute, Dalian University of Technology, Dalian 116000, China

<sup>2</sup> School of Management, Dalian University of Finance and Economics, Dalian 116000, China

\* **Correspondence:** Email: zhangc@dlut.edu.cn; Tel: +18940965007.

**Abstract:** An attempt is made in this paper to devise a finite-time adaptive fuzzy back-stepping control scheme for a class of multi-input and multi-output (MIMO) coupled nonlinear systems with immeasurable states. In view of the uncertainty of the system, adaptive fuzzy logic systems (AFLSs) are used to approach the uncertainty of the system, and the unmeasured states of the system are estimated by the finite-time extend state observers (FT-ESOs), where the state of the observer is a sphere around the state of the system. The accuracy and efficiency of the control effect are ensured by combining the back-stepping and finite-time theory. It is proved that all the states of the closed-loop adaptive control system are semi-global practical finite-time stability (SGPFS) by the finite-time Lyapunov stability theorem, and the tracking errors of the system states converge to a tiny neighborhood of the origin in a finite time. The validity of this scheme is demonstrated by a simulation.

**Keywords:** coupled nonlinear systems; adaptive fuzzy logic system; extended state observer; back-stepping; finite time

---

### **1. Introduction**

In the past few decades, nonlinear system control methods have attracted the research interest of many scholars. Moreover, the systems with complexity, uncertainty and coupling are more challenging to control. In order to achieve accurate, stable and rapid control effect, many methods have been applied to nonlinear systems, such as adaptive control, fuzzy logic control, neural network control,

back-stepping control and so on [1–6].

A new function approximator [7] is designed for strict feedback nonlinear systems, in which the unknown periodic disturbance system function is modeled by combining Fourier series and fuzzy logic systems (FLSs) to propose a tracking control approach of adaptive back-stepping. Whereas, a fuzzy adaptive back-stepping control method [8] is established for nonlinear systems with backlash hysteresis and time-varying state constraints. In order to solve the issue of differential explosion, the technique of dynamic surface control (DSC) is devised to fit a neural control or fuzzy adaptive design process for nonlinear systems with uncertain functions [9–12]. A robust adaptive fuzzy DSC is suggested for single-input and single-output (SISO) nonlinear systems with uncertainties [9]. The design process is simplified by this method while eliminating the explosion of the differential term. Moreover, some scholars use neural networks to approximate uncertain nonlinear parts. For a nonlinear system with additional interference, an adaptive back-stepping DSC approach on account of radial basis function (RBF) neural network is proposed [13]. On the other hand, for a class of uncertain SISO nonlinear systems with saturation delay and time-varying delay states, an adaptive back-stepping design scheme based on neural network is presented [14].

All the aforementioned methods are suggested for the SISO nonlinear systems. However, in the physical world, MIMO systems are most commonly used [15–20]. A control method combining FLS and back-stepping is advocated for nonlinear MIMO systems with non-measurable states [15]. An adaptive back-stepping design scheme which directly combines the output recurrent wavelet neural networks (ORWNNs) for MIMO nonlinear undefined non-affine systems is also reported [16]. A fuzzy adaptive back-stepping DSC approach [17] is put forth for MIMO with non-measurable states. An adaptive back-stepping tracking control approach using neural network [18] is suggested for interconnected mismatched systems. A fuzzy adaptive output feedback DSC are designed for stochastic systems with unmeasured states [19]. A neural network adaptive controller based on event triggering is designed for MIMO systems [20]. Although, the above studies have exhibited significant achievements for nonlinear MIMO systems with uncertainties, there is wide scope for further improvement [21–27]. On the basis of an adaptive DSC [26], the system's uncertain parts are approached by the interval type-2 fuzzy neural networks (IT2FNNs). Similarly, a flexible joint's adaptive back-stepping controller based on IT2FNN is also presented [27], where the IT2FNN controller has a smoother control surface near the steady state, which helps to improve its robustness and the ability to deal with the uncertainty in the system.

The above research literature belongs to infinite time control, with the relentless march of the technology, where the design objectives of control systems are supposed to accomplish in a finite time [28–32]. Some industrial control systems still require the controlled target within a finite time, and maintain the control effects in the systems of aircraft attitude control, robot control, multi-agent control and so on. The long transient response and the low precision performance of infinite time control methods cannot achieve such control goals. Therefore, of late, the problems of finite-time analysis have attracted the attentions of many scholars [33–39].

The finite-time adaptive neural network methods combining back-stepping are proposed for a class of uncertain nonlinear systems [33,36,38,39]. In addition, the finite-time fuzzy adaptive controllers using back-stepping have also been advocated [34,35]. Furthermore, the design of finite-time fuzzy adaptive control under event triggered strategy for un-modeled systems is studied [36]. Similarly, a finite-time fuzzy adaptive control with command filtering method for non-strict feedback systems is studied [37]. However, none of the above methods consider MIMO coupled

nonlinear system with unmeasured states. Therefore, in this paper, a finite-time adaptive fuzzy back-stepping control scheme for a class of MIMO coupled nonlinear systems with immeasurable states is devised. The solution of this issue is realized by the combination of fuzzy system, back-stepping and finite time theory.

The main advantages of this study can be summarized as follows:

- 1) The finite-time stability of MIMO nonlinear systems with uncertainty and coupling is studied by using back-stepping method, the systems are different from the non-coupled MIMO non-strict feedback system [35] and the SISO systems [36,37,39]. Since, it solves the problem that is difficult to control the non-strict feedback MIMO coupling nonlinear system with unmeasured states.
- 2) To solve the issue of the unpredictable system state, a FT-ESO is introduced to estimate the unmeasured state which fails to account for in the case where the system has unknown states [33,34,38]. Furthermore, the FT-ESO is different from the observers, where the output feedback is difficult to apply to MIMO coupling nonlinear systems [35,39].

This study not only guarantees that the observation errors converge to the tiny neighborhood of the origin in a finite time, but also ensures that the error of the system state and the reference quantity converges in a finite time. Through the finite time Lyapunov theory, it finally achieves SGPFS.

## 2. Problem formulation and preliminaries

### 2.1. System description

Considering the following nonlinear MIMO non-strict feedback system:

$$\begin{cases} \ddot{\mathbf{Q}} = \mathbf{F}(\mathbf{Q}) + \mathbf{G}(\mathbf{Q})(\mathbf{U} + \mathbf{D}) \\ \mathbf{Y} = \mathbf{Q} \end{cases} \quad (2.1)$$

Where,  $\mathbf{Q}$  is the vector of the state,  $\mathbf{Q} = [q_1 \cdots q_m]^T$ ,  $\mathbf{U}$ , and  $\mathbf{Y}$  mean the input and output variables, and  $\mathbf{D}$  is bounded disturbances represented by  $\mathbf{U} = [u_1 \ u_2 \ \cdots \ u_m]^T$ ,  $\mathbf{D} = [d_1 \ d_2 \ \cdots \ d_m]^T$ .  $\mathbf{F}(\mathbf{Q})$  and  $\mathbf{G}(\mathbf{Q})$  are unknown nonlinear smooth functions with the following structure:

$$\begin{aligned} \mathbf{F}(\mathbf{Q}) &= [f_1(\mathbf{Q}) \ f_2(\mathbf{Q}) \ \cdots \ f_m(\mathbf{Q})]^T, \\ \mathbf{G}(\mathbf{Q}) &= \begin{pmatrix} \mathbf{g}_{11}(\mathbf{Q}) & \cdots & \mathbf{g}_{12}(\mathbf{Q}) \\ \vdots & \ddots & \vdots \\ \mathbf{g}_{m1}(\mathbf{Q}) & \cdots & \mathbf{g}_{mm}(\mathbf{Q}) \end{pmatrix}, \end{aligned}$$

Remark 1: The nonlinear function  $\mathbf{F}$  and  $\mathbf{G}$  of the controlled system (2.1) are completely unknown and FLSs are used to approach the uncertainties.

Assumption 1: The total disturbance  $\mathbf{D}$  is bounded.

Assumption 2: Considering the assigned reference signals, their first-order and second-order derivatives are bounded.

### 2.2. Fuzzy approximation theory

The FLS is a form of nonlinear function and can approximate all nonlinear functions with any precision, so it can be applied to all kinds of problems. FLSs are constructed by employing some specific inference, fuzzifier and de-fuzzifier strategies and form IF-THEN rules. Consequently,

information from human experts in various fields can be integrated into the controller.

The design of a FLS is divided into four sections namely, the fuzzifier, the knowledge base, the fuzzy inference engine and the de-fuzzifier. Assuming that the FLS is composed of  $N$  fuzzy rules, the  $j^{\text{th}}$  fuzzy rule can be denoted as:

If  $x_1$  is  $F_1^j$  and  $\dots$  and  $x_n$  is  $F_n^j$ , then  $y$  is  $B^j$  ( $j = 1, 2, \dots, N$ ).

Where,  $F_1^j, B^j$  are the fuzzy sets in  $R$ , related to the membership functions.

After adopting the product Inference Engine, the singleton fuzzifier and the center average defuzzification, the FLS's output is given as:

$$y(x) = \frac{\sum_{j=1}^N \theta_j \prod_{i=1}^n \mu_i^j(x_i)}{\sum_{j=1}^N \prod_{i=1}^n \mu_i^j(x_i)} \quad (2.2)$$

Where,  $\mathbf{x} = [x_1, x_2, \dots, x_n]^T \in R^n$ ,  $\mu_i^j(x_i)$  is the membership function,  $\theta_j = \max_{y \in R} B^j(y)$ . Denote

$\boldsymbol{\varepsilon}(\mathbf{x}) = [\varepsilon_1(\mathbf{x}), \varepsilon_2(\mathbf{x}), \dots, \varepsilon_N(\mathbf{x})]^T$ ,  $\varepsilon_j(\mathbf{x})$  is fuzzy basis function,  $\varepsilon_j(\mathbf{x}) = \frac{\prod_{i=1}^n \mu_i^j(x_i)}{\sum_{j=1}^N \prod_{i=1}^n \mu_i^j(x_i)}$ . Denote

$\boldsymbol{\theta} = [\theta_1, \theta_2, \dots, \theta_N]^T$ ,  $\boldsymbol{\theta}$  is a parameter vector. Then  $\mathbf{y}(\mathbf{x}) = \boldsymbol{\varepsilon}^T(\mathbf{x})\boldsymbol{\theta}$ . A fuzzy logic system (3.20) can be constructed from (2.2) which can consistently approximate nonlinear functions to arbitrary precision.

Lemma 1. According to fuzzy universal approximation theory, if  $f(x)$  is a smooth function, and for any arbitrary constant  $\varepsilon > 0$ , there is a FLS which satisfies:  $\sup_{y \in \Omega} |f(x) - y(x)| \leq \varepsilon$ .

### 2.3. Finite Time

Lemma 2. For nonlinear systems  $\dot{\xi} = f(\xi)$ , initial values  $\xi(t) = \xi$ , if there is a constant quantity  $\varepsilon > 0$ , and a time function  $T(\varepsilon, \xi) < \infty$ , for all  $t \geq t + T_0$ , let  $\xi(t) < \varepsilon$ , then the nonlinear system's equilibrium point  $\xi = 0$  is SGPFs [40, 41].

Lemma 3. For arbitrary  $z_i \in R$ ,  $i = 1, 2, \dots, n$ , and a constant  $0 < q \leq 1$ , the following inequality is present [40,41]:

$$(\sum_{i=1}^n |z_i|)^q \leq \sum_{i=1}^n |z_i|^q \leq n^{1-q} (\sum_{i=1}^n |z_i|)^q \quad (2.3)$$

Lemma 4. For positive constants  $\mu, \delta, \iota$ , and real variables  $z, \zeta$ , the inequality is obtained as follows [41]:

$$|z|^\mu |\zeta|^\delta \leq \frac{\mu}{\mu+\delta} \iota |z|^{\mu+\delta} + \frac{\delta}{\mu+\delta} \iota^{-\frac{\mu}{\delta}} |\zeta|^{\mu+\delta} \quad (2.4)$$

Lemma 5. There is a function  $V(\xi)$  which is positive-definite, and there are constants  $c > 0$ ,  $0 < \beta < 1$ ,  $\rho > 0$ , if the nonlinear function  $\dot{\xi} = f(\xi)$  satisfies [41]:

$$\dot{V}(\xi) \leq -cV^\beta(\xi) + \rho, t \geq 0 \quad (2.5)$$

Then, the nonlinear function  $\dot{\xi} = f(\xi)$  is SGPFs.

### 3. Observer-based finite-time fuzzy adaptive back-stepping design and stability analysis

This section introduces a FT-ESO to obtain the unmeasured states [42]. Then the observer-based finite time adaptive back-stepping controller is proposed. Finally, the system's stability is verified.

#### 3.1. Finite-time extended fuzzy state observer design

Since the state of the system is unpredictable, the extended state observer needs to be designed in the following form to estimate immeasurable states:

$$\begin{aligned}\dot{\hat{\xi}}_1 &= \hat{\xi}_2 + \beta_1(t, T) \times (\xi_1 - \hat{\xi}_1) \\ \dot{\hat{\xi}}_2 &= \hat{\xi}_3 + \beta_2(t, T) \times (\xi_1 - \hat{\xi}_1) \\ \dot{\hat{\xi}}_\rho &= \hat{\xi}_{\rho+1} + \beta_\rho(t, T) \times (\xi_1 - \hat{\xi}_1) + u \\ \dot{\hat{\xi}}_{\rho+1} &= \beta_{\rho+1}(t, T) \times (\xi_1 - \hat{\xi}_1)\end{aligned}\quad (3.1)$$

Where, the time-varying gains  $\beta_i(t, T)$  are functions of a constant parameter  $T$  and the real-time  $t$ . The convergence time is regulated by select parameter  $T$  later. The vector of estimation error is defined as:  $e = \xi - \hat{\xi}$ . The error models are generated as follows:

$$\begin{aligned}\dot{e}_i &= e_{i+1} - \beta_i \times e_1 \\ \dot{e}_{\rho+1} &= S - \beta_{\rho+1} \times e_1\end{aligned}\quad (3.2)$$

In order to weaken the errors  $e_i$  to a tiny area of 0 along with  $t$  incline to the convergence time  $T$ , the time-varying gains will be given. Considering nonlinear system (2.1) and the observer (3.1), which derive the error model (3.2), the extended state observer gains  $\beta_i$  are presented as follows:

$$\beta_i = L_i + \bar{\beta}_{i,1} \frac{\rho+i}{2T} (1 - \mu_1^{-1}) \mu_1^{i-1} - \bar{\beta}_{i+1,1} \mu_1^i - \sum_{j=1}^{i-1} \bar{\beta}_{i,j} \mu_1^{i-j} \beta_j, \quad i = 1, 2, \dots, \rho \quad (3.3)$$

$$\beta_{\rho+1} = L_{\rho+1} + \bar{\beta}_{\rho+1,1} \frac{2\rho+1}{2T} (1 - \mu_1^{-1}) \mu_1^\rho - \sum_{j=1}^\rho \bar{\beta}_{\rho+1,j} \mu_1^{\rho-j+1} \beta_j \quad (3.4)$$

Where,  $\bar{\beta}_{i,j}$  for  $i = 1, 2, \dots, \rho$  and  $j = 2, \dots, \rho + 1$  are given as follows:

$$\bar{\beta}_{i,j-1} = \beta_{i,j} \frac{\rho+1}{2T} (1 + \mu_1^{-1}) \mu_1^{-1} + \bar{\beta}_{i,j} \frac{i-j}{2T} (1 - \mu_1^{-1}) \mu_1^{-1} + \bar{\beta}_{i+1,j} \quad (3.5)$$

$i = 2, \dots, \rho. \quad j = 2, \dots, \rho + 1.$

Moreover,

$$\bar{\beta}_{\rho+1,j-1} = \bar{\beta}_{\rho+1,j} \frac{\rho+1}{2T} (1 + \mu_1^{-1}) \mu_1^{-1} + \bar{\beta}_{\rho+1,j} \frac{\rho-j+1}{2T} (1 - \mu_1^{-1}) \mu_1^{-1} \quad (3.6)$$

Where,  $\bar{\beta}_{i,i} = 1$  and for  $i < j$  one has  $\bar{\beta}_{i,j} = 0$ ,  $\mu_1(t, T) = \frac{1+e^{-\frac{t}{T}}}{2e^{-\frac{t}{T}}}$ . The scalar coefficients  $\{L_i\}$  for

$$i = 1, \dots, \rho \text{ are chosen such that the } (\rho + 1) \times (\rho + 1) \text{ matrix } \Lambda = \begin{bmatrix} -L_1 & 1 & \dots & 0 \\ \vdots & \vdots & \ddots & 0 \\ -L_\rho & 0 & \ddots & 1 \\ -L_{\rho+1} & 0 & \dots & 0 \end{bmatrix} \text{ satisfies Hurwitz.}$$

The error model (3.2) is stable along with the time  $T$  of convergence and the error model (3.2) is finite-time input-to-state stable (FT-ISS) for a positive constant  $\varepsilon > 1$ ,

$$\|e\| \leq v^{m+1} \sup_t \|\Gamma(v)\| \left[ \varepsilon e^{At} \|\beta(1)\| \|e(0)\| + \int_0^t e^{A(t-\tau)} \|B\| \mu |S| d\tau \right] \quad (3.7)$$

Where,  $\mu(t, T) = \mu_1^{\rho+1}$ , and  $v(t, T) = \mu_1^{-1}$  are time-varying functions. Moreover, gradually  $B = [0 \dots 0 \ 1]$ ,  $m$  is an integer design parameter,  $\beta$  is a lower triangular matrix. Moreover,  $\Gamma(v)$  is defined as  $\beta^{-1}$ .

The Lyapunov function is chosen as  $V_0 = \frac{1}{2} \sum_{j=1}^2 e_j^2$ , after differentiating, we get the following formula:  $\dot{V}_0 \leq -c_k V_0^\alpha$ .

Remark 2: The estimation error is equally bounded in finite time by the scheme without knowing the upper bound of the perturbation. Then, using the finite-time Lyapunov function described in the next part, a controller is built to maintain the closed-loop system's stability.

### 3.2. Finite-time adaptive back-stepping design and stability analysis

In this part, a finite-time adaptive fuzzy control approach is proposed by the adaptive back-stepping technique and the stability analysis is shown through the finite-time Lyapunov function.

The system is converted as follows to apply back-stepping technique:

$$\begin{cases} \dot{x}_1 = x_2 \\ \dot{x}_2 = F(x_1, x_2) + G(x_1, x_2)(U + D) \\ y = x_1 \end{cases} \quad (3.8)$$

Where,  $x_1 = Q$ ,  $x_2 = \dot{Q}$ .

Step 1: Define position vector error:

$$z_1 = \hat{x}_1 - x_{1d} \quad (3.9)$$

Where,  $x_{1d}$  is the reference signal.

$$\dot{z}_1 = \hat{\dot{x}}_1 - \dot{x}_{1d} \quad (3.10)$$

$$z_2 = \hat{x}_2 - \alpha_1 \quad (3.11)$$

Define virtual control quantity

$$\alpha_1 = -c_1 z_1 (z_1^T z_1)^{\beta-1} + \dot{x}_{1d} \quad (3.12)$$

Where,  $c_1 > 0$ . For the singularity problem in the subsequent derivation of  $\alpha_1$ , the method of obtaining the pseudo-inverse matrix is used to solve it. The differential expression is  $\dot{\alpha}_1 =$

$-\mathbf{c}_1 \dot{\mathbf{z}}_1 (\mathbf{z}_1^T \mathbf{z}_1)^{-1 \cdot (1-\beta)} - 2\mathbf{c}_1 (\beta - 1) \mathbf{z}_1 (\mathbf{z}_1^T \mathbf{z}_1)^{-1 \cdot (2-\beta)} \dot{\mathbf{z}}_1^T \mathbf{z}_1$ . When  $\mathbf{z}_1^T \mathbf{z}_1 = 0$ ,  $0 < \beta < 1$ ,  $(\mathbf{z}_1^T \mathbf{z}_1)^{-1 \cdot (1-\beta)}$  has a singularity problem, so the pseudo inverse value needs to be obtained, and then  $(\mathbf{z}_1^T \mathbf{z}_1)^{-1 \cdot (1-\beta)} = \mathbf{0}$ . There are similar problems in  $(\mathbf{z}_1^T \mathbf{z}_1)^{-1 \cdot (2-\beta)}$ , therefore, it will not be repeated. After the above analysis, the value at the singularity is  $\dot{\boldsymbol{\alpha}}_1 = \mathbf{0}$ .

For the first subsystem, considering the observer stability and position errors, define Lyapunov function as:

$$\mathbf{V}_1 = \mathbf{V}_0 + \frac{1}{2} \mathbf{z}_1^T \mathbf{z}_1 \quad (3.13)$$

When the estimation matrix  $\mathbf{G}$  is singular, the above operation is difficult to achieve. In order to overcome this disadvantage, we find the generalized inverse of  $\mathbf{G}$ . Then,

$$\begin{aligned} \dot{\mathbf{V}}_1 = \mathbf{z}_1^T (\mathbf{z}_2 + \boldsymbol{\alpha}_1 - \dot{\mathbf{x}}_{1d}) + \dot{\mathbf{V}}_0 = \mathbf{z}_1^T [\mathbf{z}_2 - \mathbf{c}_1 \mathbf{z}_1 (\mathbf{z}_1^T \mathbf{z}_1)^{\beta-1}] + \dot{\mathbf{V}}_0 = \mathbf{z}_1^T \mathbf{z}_2 - \\ \mathbf{c}_1 (\mathbf{z}_1^T \mathbf{z}_1)^\beta + \dot{\mathbf{V}}_0 \end{aligned} \quad (3.14)$$

If  $\mathbf{z}_2 = 0$ , then  $\dot{\mathbf{V}}_1 \leq 0$ .

Step 2: Design controller:

$$\dot{\mathbf{z}}_2 = \dot{\mathbf{x}}_2 - \dot{\boldsymbol{\alpha}}_1 = \mathbf{F}(\hat{\mathbf{x}}_1, \hat{\mathbf{x}}_2) + \mathbf{G}(\hat{\mathbf{x}}_1, \hat{\mathbf{x}}_2)(\mathbf{U} + \mathbf{D}) - \dot{\boldsymbol{\alpha}}_1 \quad (3.15)$$

For the second subsystem, considering speed errors, define Lyapunov function as

$$\mathbf{V}_2 = \mathbf{V}_1 + \frac{1}{2} \mathbf{z}_2^T \mathbf{G}^{-1} \mathbf{z}_2 \quad (3.16)$$

Then,

$$\begin{aligned} \dot{\mathbf{V}}_2 = \dot{\mathbf{V}}_0 + \dot{\mathbf{V}}_1 + \frac{1}{2} \mathbf{z}_2^T \mathbf{G}^{-1} \dot{\mathbf{z}}_2 + \frac{1}{2} \dot{\mathbf{z}}_2^T \mathbf{G}^{-1} \mathbf{z}_2 + \frac{1}{2} \mathbf{z}_2^T \dot{\mathbf{G}}^{-1} \mathbf{z}_2 = \mathbf{z}_1^T \mathbf{z}_2 - \mathbf{c}_1 (\mathbf{z}_1^T \mathbf{z}_1)^\beta + \mathbf{z}_2^T \mathbf{G}^{-1} \dot{\mathbf{z}}_2 + \\ \frac{1}{2} \mathbf{z}_2^T \dot{\mathbf{G}}^{-1} \mathbf{z}_2 + \dot{\mathbf{V}}_0 = \mathbf{z}_1^T \mathbf{z}_2 - \mathbf{c}_1 (\mathbf{z}_1^T \mathbf{z}_1)^\beta + \mathbf{z}_2^T \mathbf{G}^{-1} [\mathbf{F} + \mathbf{G}(\mathbf{U} + \mathbf{D}) - \dot{\boldsymbol{\alpha}}_1] + \frac{1}{2} \mathbf{z}_2^T \dot{\mathbf{G}}^{-1} \mathbf{z}_2 + \dot{\mathbf{V}}_0 = \\ \mathbf{z}_1^T \mathbf{z}_2 - \mathbf{c}_1 (\mathbf{z}_1^T \mathbf{z}_1)^\beta + \mathbf{z}_2^T (\mathbf{G}^{-1} \mathbf{F} + \mathbf{U} + \mathbf{D} - \mathbf{G}^{-1} \dot{\boldsymbol{\alpha}}_1) + \frac{1}{2} \mathbf{z}_2^T \dot{\mathbf{G}}^{-1} \mathbf{z}_2 + \dot{\mathbf{V}}_0 = \mathbf{z}_1^T \mathbf{z}_2 - \\ \mathbf{c}_1 (\mathbf{z}_1^T \mathbf{z}_1)^\beta + \mathbf{z}_2^T (\mathbf{G}^{-1} \mathbf{F} + \mathbf{U} - \mathbf{G}^{-1} \dot{\boldsymbol{\alpha}}_1 + \frac{1}{2} \dot{\mathbf{G}}^{-1} \mathbf{z}_2) + \mathbf{z}_2^T \mathbf{D} + \dot{\mathbf{V}}_0 \end{aligned} \quad (3.17)$$

Let  $\mathbf{f} = \mathbf{G}^{-1} \mathbf{F} - \mathbf{G}^{-1} \dot{\boldsymbol{\alpha}}_1 + \frac{1}{2} \dot{\mathbf{G}}^{-1} \mathbf{z}_2$ .

It can be seen from the expression of  $\mathbf{f}$ , that  $\mathbf{f}$  contains the model information of the above systems. In order to realize the control without model information, FLS is used to approximate  $\mathbf{f}$ .

Based on Lemma 1, we expect that the continuous function  $\mathbf{f}$  can be evaluated by the FLS as following

$$\varphi_1(\hat{\mathbf{x}}) = \frac{\sum_{i=1}^N \theta_{1i} \prod_{j=1}^n \mu_j^i(\hat{x}_j)}{\sum_{i=1}^N [\prod_{j=1}^n \mu_j^i(\hat{x}_j)]} = \boldsymbol{\varepsilon}_1^T \boldsymbol{\theta}_1 \quad (3.18)$$

$$\varphi_2(\hat{\boldsymbol{x}}) = \frac{\sum_{i=1}^N \theta_{2i} \prod_{j=1}^n \mu_j^i(\hat{x}_j)}{\sum_{i=1}^N [\prod_{j=1}^n \mu_j^i(\hat{x}_j)]} = \boldsymbol{\varepsilon}_2^T \boldsymbol{\theta}_2 \quad (3.19)$$

Define

$$\boldsymbol{\varphi} = \boldsymbol{\varepsilon}^T(\hat{\boldsymbol{x}}) \boldsymbol{\theta} \quad (3.20)$$

Deform the above formula (3.20) into

$$\boldsymbol{\varphi} = [\varphi_1, \varphi_2]^T = \begin{bmatrix} \boldsymbol{\varepsilon}_1^T & 0 \\ 0 & \boldsymbol{\varepsilon}_2^T \end{bmatrix} \begin{bmatrix} \boldsymbol{\theta}_1 \\ \boldsymbol{\theta}_2 \end{bmatrix} = \boldsymbol{\varepsilon}^T(\hat{\boldsymbol{x}}) \boldsymbol{\theta} \quad (3.21)$$

Where,  $\boldsymbol{\varphi}$ ,  $\hat{\boldsymbol{x}}$  are the estimation of  $\boldsymbol{f}$ ,  $\boldsymbol{x}$ . And  $\varepsilon_i(\hat{\boldsymbol{x}}) = \frac{\prod_{j=1}^n \mu_j^i(\hat{x}_j)}{\sum_{i=1}^N [\prod_{j=1}^n \mu_j^i(\hat{x}_j)]}$ .

Then, we design control rate as

$$\boldsymbol{U} = -\boldsymbol{c}_2 \boldsymbol{z}_2 (\boldsymbol{z}_2^T \boldsymbol{z}_2)^{\beta-1} - \boldsymbol{z}_1 - \boldsymbol{\varphi} - \boldsymbol{z}_2 \quad (3.22)$$

Substituting (3.18), (3.19) into (3.17), we have

$$\begin{aligned} \dot{\boldsymbol{V}}_2 &= \boldsymbol{z}_1^T \boldsymbol{z}_2 - \boldsymbol{c}_1 (\boldsymbol{z}_1^T \boldsymbol{z}_1)^\beta + \boldsymbol{z}_2^T (\boldsymbol{f} + \boldsymbol{U}) + \boldsymbol{z}_2^T \boldsymbol{D} + \dot{\boldsymbol{V}}_0 = -\boldsymbol{c}_1 (\boldsymbol{z}_1^T \boldsymbol{z}_1)^\beta - \boldsymbol{c}_2 (\boldsymbol{z}_2^T \boldsymbol{z}_2)^\beta + \\ \boldsymbol{z}_2^T (\boldsymbol{f} - \boldsymbol{\varphi}) + \boldsymbol{z}_2^T \boldsymbol{D} - \boldsymbol{z}_2^T \boldsymbol{z}_2 + \dot{\boldsymbol{V}}_0 &= -\boldsymbol{c}_1 (\boldsymbol{z}_1^T \boldsymbol{z}_1)^\beta - \boldsymbol{c}_2 (\boldsymbol{z}_2^T \boldsymbol{z}_2)^\beta + \boldsymbol{z}_2^T (\boldsymbol{f} - \boldsymbol{\varepsilon}(\hat{\boldsymbol{x}}) \boldsymbol{\theta}) + \boldsymbol{z}_2^T \boldsymbol{D} - \\ &\boldsymbol{z}_2^T \boldsymbol{z}_2 + \dot{\boldsymbol{V}}_0 \end{aligned} \quad (3.23)$$

Step 3: Stability analysis:

For smooth function  $\boldsymbol{f}$ , there is an optimal constant  $\boldsymbol{\theta}^*$  that minimizes the approximation error. Define the optimal constant as

$$\boldsymbol{\theta}^* = \underset{\boldsymbol{\theta} \in \Omega_0}{\operatorname{argmin}} \left[ \sup_{\boldsymbol{x} \in \Omega} |\boldsymbol{f} - \boldsymbol{\varepsilon}(\hat{\boldsymbol{x}}) \boldsymbol{\theta}| \right] \quad (3.24)$$

Where,  $\Omega_0$  and  $\Omega$  is bounded set.

The approximation constant error is

$$\tilde{\boldsymbol{\theta}} = \boldsymbol{\theta}^* - \boldsymbol{\theta} \quad (3.25)$$

Considering the whole system, define Lyapunov function as

$$\boldsymbol{V}_3 = \boldsymbol{V}_2 + \frac{1}{2\gamma} \tilde{\boldsymbol{\theta}}^T \tilde{\boldsymbol{\theta}} \quad (3.26)$$

Where,  $\gamma > 0$ . Then,

$$\begin{aligned} \dot{\boldsymbol{V}}_3 &= \dot{\boldsymbol{V}}_2 - \frac{1}{\gamma} \tilde{\boldsymbol{\theta}}^T \dot{\boldsymbol{\theta}} = -\boldsymbol{c}_1 (\boldsymbol{z}_1^T \boldsymbol{z}_1)^\beta - \boldsymbol{c}_2 (\boldsymbol{z}_2^T \boldsymbol{z}_2)^\beta + \boldsymbol{z}_2^T (\boldsymbol{f} - \boldsymbol{\varepsilon}(\hat{\boldsymbol{x}}) \boldsymbol{\theta}) + \boldsymbol{z}_2^T \boldsymbol{D} - \boldsymbol{z}_2^T \boldsymbol{z}_2 - \frac{1}{\gamma} \tilde{\boldsymbol{\theta}}^T \dot{\boldsymbol{\theta}} + \\ \dot{\boldsymbol{V}}_0 &= -\boldsymbol{c}_1 (\boldsymbol{z}_1^T \boldsymbol{z}_1)^\beta - \boldsymbol{c}_2 (\boldsymbol{z}_2^T \boldsymbol{z}_2)^\beta + \boldsymbol{z}_2^T (\boldsymbol{f} - \boldsymbol{\varepsilon}(\hat{\boldsymbol{x}}) \boldsymbol{\theta}^*) + \boldsymbol{z}_2^T (\boldsymbol{\varepsilon}(\hat{\boldsymbol{x}}) \boldsymbol{\theta}^* - \boldsymbol{\varepsilon}(\hat{\boldsymbol{x}}) \boldsymbol{\theta}) + \boldsymbol{z}_2^T \boldsymbol{D} - \frac{1}{\gamma} \tilde{\boldsymbol{\theta}}^T \dot{\boldsymbol{\theta}} - \\ &\boldsymbol{z}_2^T \boldsymbol{z}_2 + \dot{\boldsymbol{V}}_0 \end{aligned} \quad (3.27)$$

According to the matrix norm inequality, we get  $\|\boldsymbol{z}_2^T (\boldsymbol{f} - \boldsymbol{\varepsilon}(\hat{\boldsymbol{x}}) \boldsymbol{\theta})\| \leq \|\boldsymbol{z}_2^T\| \cdot \|\boldsymbol{f} - \boldsymbol{\varepsilon}(\hat{\boldsymbol{x}}) \boldsymbol{\theta}^*\|$ ,  $\|\boldsymbol{z}_2^T \boldsymbol{D}\| \leq \|\boldsymbol{z}_2^T\| \cdot \|\boldsymbol{D}\|$ . Then, transform (3.27) into the following form:



$$\dot{V}_3 \leq -c_1(\mathbf{z}_1^T \mathbf{z}_1)^\beta - c_2(\mathbf{z}_2^T \mathbf{z}_2)^\beta + \|\mathbf{z}_2^T\| \cdot \|\mathbf{f} - \boldsymbol{\varepsilon}(\hat{\mathbf{x}})\boldsymbol{\theta}^*\| + \mathbf{z}_2^T \boldsymbol{\varepsilon}(\hat{\mathbf{x}})\tilde{\boldsymbol{\theta}} - \frac{1}{\gamma}\tilde{\boldsymbol{\theta}}^T \dot{\boldsymbol{\theta}} + \|\mathbf{z}_2^T\| \cdot \|\mathbf{D}\| - \mathbf{z}_2^T \mathbf{z}_2 + \dot{V}_0 \quad (3.28)$$

According to Young's inequality, the transformation of (3.28) is as follows

$$\dot{V}_3 \leq -c_1(\mathbf{z}_1^T \mathbf{z}_1)^\beta - c_2(\mathbf{z}_2^T \mathbf{z}_2)^\beta + \frac{1}{2}\|\mathbf{z}_2^T\|^2 + \frac{1}{2}\epsilon^2 + \tilde{\boldsymbol{\theta}}[\mathbf{z}_2^T \boldsymbol{\varepsilon}(\hat{\mathbf{x}}) - \frac{1}{\gamma}\dot{\boldsymbol{\theta}}] + \frac{1}{2}\|\mathbf{z}_2^T\|^2 + \frac{1}{2}\|\mathbf{D}\|^2 - \mathbf{z}_2^T \mathbf{z}_2 + \dot{V}_0 \quad (3.29)$$

Design adaptive law as:

$$\dot{\boldsymbol{\theta}} = \gamma(\mathbf{z}_2^T \boldsymbol{\varepsilon}(\hat{\mathbf{x}}))^T - 2k\boldsymbol{\theta}, \quad \gamma \geq 0 \quad (3.30)$$

Substituting (3.29) into (3.30), we have

$$\begin{aligned} \dot{V}_3 &= -c_1(\mathbf{z}_1^T \mathbf{z}_1)^\beta - c_2(\mathbf{z}_2^T \mathbf{z}_2)^\beta + \|\mathbf{z}_2^T\|^2 + \frac{1}{2}\epsilon^2 + \tilde{\boldsymbol{\theta}}^T \frac{2k\boldsymbol{\theta}}{\gamma} + \frac{1}{2}\|\mathbf{D}\|^2 - \mathbf{z}_2^T \mathbf{z}_2 + \dot{V}_0 \leq \\ &-c_1(\mathbf{z}_1^T \mathbf{z}_1)^\beta - c_2(\mathbf{z}_2^T \mathbf{z}_2)^\beta + \mathbf{z}_2^T \mathbf{z}_2 + \frac{1}{2}\epsilon^2 + \frac{k}{\gamma}(2\boldsymbol{\theta}^{*T}\boldsymbol{\theta} - 2\boldsymbol{\theta}^T\boldsymbol{\theta}) + \frac{1}{2}\mathbf{D}^T\mathbf{D} - \mathbf{z}_2^T \mathbf{z}_2 + \dot{V}_0 \end{aligned} \quad (3.31)$$

From  $(\boldsymbol{\theta} - \boldsymbol{\theta}^*)^T(\boldsymbol{\theta} - \boldsymbol{\theta}^*) \geq 0$ , we can get

$$2\boldsymbol{\theta}^{*T}\boldsymbol{\theta} - 2\boldsymbol{\theta}^T\boldsymbol{\theta} \leq -\boldsymbol{\theta}^T\boldsymbol{\theta} + \boldsymbol{\theta}^{*T}\boldsymbol{\theta} \quad (3.32)$$

Take (3.32) into the (3.31) and we get

$$\begin{aligned} \dot{V}_3 &\leq -c_1(\mathbf{z}_1^T \mathbf{z}_1)^\beta - c_2(\mathbf{z}_2^T \mathbf{z}_2)^\beta + \frac{1}{2}\epsilon^2 + \frac{k}{\gamma}(\boldsymbol{\theta}^{*T}\boldsymbol{\theta}^* - \boldsymbol{\theta}^T\boldsymbol{\theta}) + \frac{1}{2}\mathbf{D}^T\mathbf{D} + \dot{V}_0 \leq -c_1(\mathbf{z}_1^T \mathbf{z}_1)^\beta - \\ &c_2(\mathbf{z}_2^T \mathbf{z}_2)^\beta + \frac{1}{2}\epsilon^2 - \frac{k}{2\gamma}\tilde{\boldsymbol{\theta}}^T\tilde{\boldsymbol{\theta}} + \frac{2k}{\gamma}\boldsymbol{\theta}^{*T}\boldsymbol{\theta}^* + \dot{V}_0 + \frac{1}{2}\mathbf{D}^T\mathbf{D} \end{aligned} \quad (3.33)$$

From  $(\boldsymbol{\theta} + \boldsymbol{\theta}^*)^T(\boldsymbol{\theta} + \boldsymbol{\theta}^*) \geq 0$ , we can get

$$-\boldsymbol{\theta}^{*T}\boldsymbol{\theta} - \boldsymbol{\theta}^T\boldsymbol{\theta}^* \leq \boldsymbol{\theta}^T\boldsymbol{\theta} + \boldsymbol{\theta}^{*T}\boldsymbol{\theta}^* \quad (3.34)$$

Furthermore, we derive

$$-\boldsymbol{\theta}^T\boldsymbol{\theta} - \boldsymbol{\theta}^{*T}\boldsymbol{\theta}^* \leq -\frac{1}{2}\tilde{\boldsymbol{\theta}}^T\tilde{\boldsymbol{\theta}} \quad (3.35)$$

Then, substituting (3.35) into (3.33), we have

$$\dot{V}_3 = -c_1(\mathbf{z}_1^T \mathbf{z}_1)^\beta - c_2(\mathbf{z}_2^T \mathbf{z}_2)^\beta - \frac{k}{2\gamma}\tilde{\boldsymbol{\theta}}^T\tilde{\boldsymbol{\theta}} + \frac{1}{2}\epsilon^2 + \frac{2k}{\gamma}\boldsymbol{\theta}^{*T}\boldsymbol{\theta}^* + \frac{1}{2}\mathbf{D}^T\mathbf{D} + \dot{V}_0 \quad (3.36)$$

In order to deal with terms  $\frac{k}{2\gamma}\tilde{\boldsymbol{\theta}}^T\tilde{\boldsymbol{\theta}}$ ,

$$\begin{aligned} \dot{V}_3 &= -c_1(\mathbf{z}_1^T \mathbf{z}_1)^\beta - c_2(\mathbf{z}_2^T \mathbf{z}_2)^\beta - \frac{k}{2\gamma}\tilde{\boldsymbol{\theta}}^T\tilde{\boldsymbol{\theta}} + \frac{k}{2\gamma}(\tilde{\boldsymbol{\theta}}^T\tilde{\boldsymbol{\theta}})^\beta - \frac{k}{2\gamma}(\tilde{\boldsymbol{\theta}}^T\tilde{\boldsymbol{\theta}})^\beta + \frac{1}{2}\epsilon^2 + \frac{2k}{\gamma}\boldsymbol{\theta}^{*T}\boldsymbol{\theta}^* + \\ &\frac{1}{2}\mathbf{D}^T\mathbf{D} + \dot{V}_0 \end{aligned} \quad (3.37)$$

Now, by using Lemma 4,  $z = 1$ , select designed parameters as  $\boldsymbol{\mu} = \mathbf{1} - \boldsymbol{\beta}$ ,  $\boldsymbol{\delta} = \boldsymbol{\beta}$ ,  $\boldsymbol{\iota} = \boldsymbol{\beta}^{\frac{\beta}{1-\beta}}$ , respectively, we get the following inequality

$$(\tilde{\boldsymbol{\theta}}^T \tilde{\boldsymbol{\theta}})^\beta \leq (\mathbf{1} - \boldsymbol{\beta})\boldsymbol{\iota} + \tilde{\boldsymbol{\theta}}^T \tilde{\boldsymbol{\theta}} \quad (3.38)$$

Substituting (3.38) into (3.37), we have

$$\begin{aligned} \dot{V}_3 \leq & -c_1(\mathbf{z}_1^T \mathbf{z}_1)^\beta - c_2(\mathbf{z}_2^T \mathbf{z}_2)^\beta - \frac{k}{2\gamma} \tilde{\boldsymbol{\theta}}^T \tilde{\boldsymbol{\theta}} + \frac{k}{2\gamma} (\mathbf{1} - \boldsymbol{\beta})\boldsymbol{\iota} + \frac{k}{2\gamma} \tilde{\boldsymbol{\theta}}^T \tilde{\boldsymbol{\theta}} - \frac{k}{2\gamma} (\tilde{\boldsymbol{\theta}}^T \tilde{\boldsymbol{\theta}})^\beta + \frac{1}{2} \boldsymbol{\epsilon}^2 + \\ & \frac{2k}{\gamma} \boldsymbol{\theta}^{*T} \boldsymbol{\theta}^* + \frac{1}{2} \mathbf{D}^T \mathbf{D} + \dot{V}_0 \end{aligned} \quad (3.39)$$

Let  $\mathbf{z}_2^T \mathbf{z}_2 \leq \sigma \mathbf{z}_2^T \mathbf{G}^{-1} \mathbf{z}_2$ , then we can have

$$\begin{aligned} \dot{V}_3 \leq & -c_1(\mathbf{z}_1^T \mathbf{z}_1)^\beta - c_2(\sigma \mathbf{z}_2^T \mathbf{G}^{-1} \mathbf{z}_2)^\beta - \frac{k}{2\gamma} (\tilde{\boldsymbol{\theta}}^T \tilde{\boldsymbol{\theta}})^\beta + \frac{k}{2\gamma} (\mathbf{1} - \boldsymbol{\beta})\boldsymbol{\iota} + \frac{1}{2} \boldsymbol{\epsilon}^2 + \frac{2k}{\gamma} \boldsymbol{\theta}^{*T} \boldsymbol{\theta}^* + \frac{1}{2} \mathbf{D}^T \mathbf{D} + \\ \dot{V}_0 \leq & -c_1 2^\beta \left(\frac{1}{2} \mathbf{z}_1^T \mathbf{z}_1\right)^\beta - c_2 \sigma^\beta 2^\beta \left(\frac{1}{2} \mathbf{z}_2^T \mathbf{G}^{-1} \mathbf{z}_2\right)^\beta - \frac{k}{2\gamma} (2\gamma)^\beta \left(\frac{1}{2\gamma} \tilde{\boldsymbol{\theta}}^T \tilde{\boldsymbol{\theta}}\right)^\beta + \frac{k}{2\gamma} (\mathbf{1} - \boldsymbol{\beta})\boldsymbol{\iota} + \frac{1}{2} \boldsymbol{\epsilon}^2 + \\ & \frac{2k}{\gamma} \boldsymbol{\theta}^{*T} \boldsymbol{\theta}^* + \frac{1}{2} \mathbf{D}^T \mathbf{D} + \dot{V}_0 \end{aligned} \quad (3.40)$$

Then, choosing  $A = \min\left\{c_1 2^\beta, c_2 \sigma^\beta 2^\beta, \frac{k}{2\gamma} (2\gamma)^\beta\right\}$  and using Lemma 3, (3.40) can be rewritten as:

$$\dot{V}_3 \leq -AV_3^\beta + B \quad (3.41)$$

Where,  $B = \frac{k}{2\gamma} (\mathbf{1} - \boldsymbol{\beta})\boldsymbol{\iota} + \frac{1}{2} \boldsymbol{\epsilon}^2 + \frac{2k}{\gamma} \boldsymbol{\theta}^{*T} \boldsymbol{\theta}^* + \frac{1}{2} \mathbf{D}^T \mathbf{D}$ .

Now, the design step of the controller is accomplished. The analysis result is shown below:

Theorem 1: Considering that the system (2.1) and the Lemmas 1–5, closed-loop system signals are bounded under the controller (3.22), FT-ESO (3.1), and the intermediate control functions (3.12), parameter adaptive laws (3.30). Now we prove it.

Define the reach time  $T_r$  as

$$T_r = \frac{1}{A(1-\beta)} \left[ V^{1-\beta}(\zeta(0)) - \left(\frac{B}{A(1-\eta)}\right)^{\frac{1-\beta}{\beta}} \right] \quad (3.42)$$

Where,  $V(\zeta(0))$  is the initial value. Then, in the light of Lemma 5,  $V^\beta(\zeta) \leq \frac{B}{(1-\eta)A}$ , for  $\forall t \geq T_r$ .

This indicates that all the closed-loop state variables are SGPFs. Furthermore, the following inequality shows the tracking error gets into a tiny neighborhood around the origin after the  $T_r$ .

$$|\mathbf{y} - \mathbf{y}_d| \leq 2 \left(\frac{B}{A(1-\eta)}\right)^{\frac{1}{2\beta}} \quad (3.43)$$

Remark 3: The selection of the designed controller parameters is directly related to the capability of the dynamic response. Decreasing the neighborhood radius and increasing the convergence speed of the state vectors in system (2.1) is accomplished by increasing the parameter values. However, this leads to a greater control input that the designed parameters gain through trial-and-error method. We should gradually enlarge them from zero until the performance is contented. The structure of the above design approach is displayed in Figure 1.

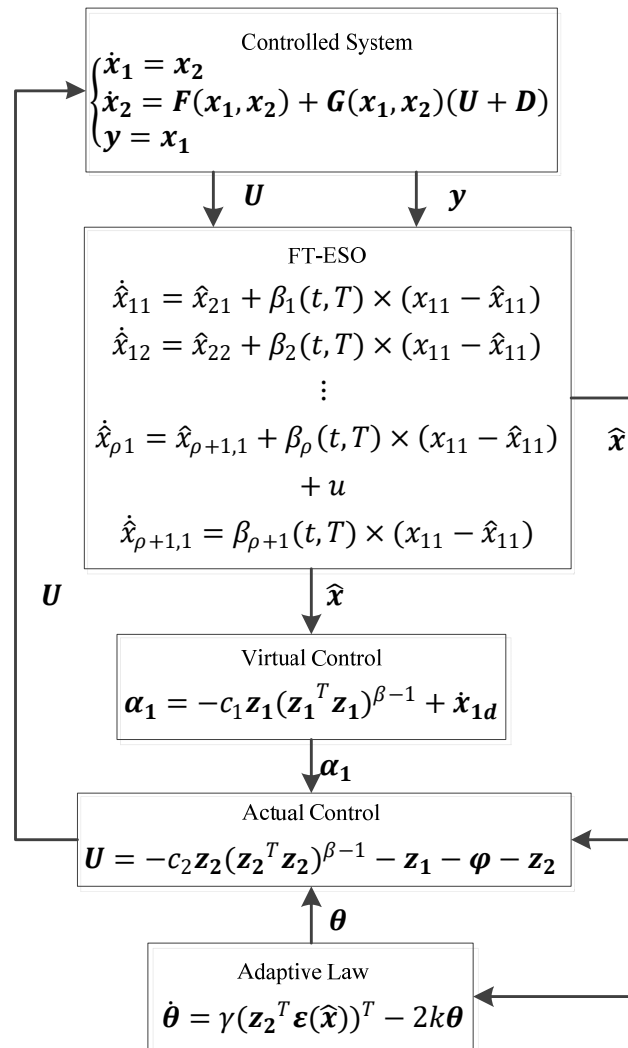


Figure 1. Block diagram of the finite-time control strategy.

#### 4. Simulation study

In this section, the simulation example is considered to prove the validity of the presented control scheme. Dynamic model of the two-joint manipulator system is given as:

$$\begin{bmatrix} \ddot{q}_1 \\ \ddot{q}_2 \end{bmatrix} = \begin{bmatrix} H_{11} & H_{12} \\ H_{21} & H_{22} \end{bmatrix}^{-1} \left( \begin{bmatrix} C_{11} & C_{12} \\ C_{21} & C_{22} \end{bmatrix} \begin{bmatrix} \dot{q}_1 \\ \dot{q}_2 \end{bmatrix} + \begin{bmatrix} u_1 \\ u_2 \end{bmatrix} + \begin{bmatrix} d_1 \\ d_2 \end{bmatrix} \right) \quad (4.1)$$

Where,  $H_{11} = J_1 + J_2 + 2m_2 r_2 l_1 \cos(q_2)$ ,  $H_{12} = H_{21} = J_2 + m_2 r_2 l_1 \cos(q_2)$ ,  $H_{22} = J_2$ ,  $C_{11} =$

$-2m_2r_2l_1\dot{\theta}_2 \sin(\theta_2)$  ,  $C_{12} = -m_2r_2l_1\dot{\theta}_2 \sin(\theta_2)$  ,  $C_{21} = m_2r_2l_1\dot{\theta}_1 \sin(\theta_2)$  ,  $C_{22} = 0$  ,  $J_1 = \frac{4}{3}m_1r_1^2 + m_2l_1^2$  ,  $J_2 = \frac{4}{3}m_2r_2^2$  ,  $m_1$  is the first link mass,  $m_2$  is the second link mass,  $l_1$  is the first link length,  $r_1$ ,  $r_2$  are the length from the joint to the gravity center of the corresponding link,  $q_1$ ,  $q_2$  are the angle of the first link and second link respectively,  $u_1$ ,  $u_2$  are the input signals of the two joints,  $J_1$  is the inertia of the first link,  $J_2$  is the inertia of the second link respectively. Taking the system parameter as  $m_1 = 0.765$ ,  $m_2 = 0.765$ ,  $l_2 = 0.25$ ,  $r_1 = 0.15$ ,  $r_2 = 0.15$ ,  $d_1 = 0.25 \sin t$ ,  $d_2 = 0.25 \sin t$ .

The state initial value of the system is  $x(0) = [0.2, 0.2, 0, 0]$ . The designed parameters are  $c_{11} = 10$ ,  $c_{21} = 15$ ,  $k_1 = 1.5$ ,  $\gamma_1 = 2$ ,  $c_{12} = 2$ ,  $c_{22} = 2.5$ ,  $k_2 = 1.5$ ,  $\gamma_2 = 2$ . The desired trajectory is  $y_{1d} = y_{2d} = \sin(2\pi t)$ .

Three fuzzy sets are selected for each variable therefore there are 12 fuzzy rules in total, choosing the following fuzzy membership functions as:

$$\begin{aligned}\mu_i^1 &= \exp[-0.5((x_i + 1.25)/0.6)^2], \\ \mu_i^2 &= \exp[-0.5((x_i)/0.6)^2], \\ \mu_i^3 &= \exp\left[-0.5\left(\frac{x_i - 1.25}{0.6}\right)^2\right], i = 1, 2, 3, 4.\end{aligned}$$

Based on the system, the FT-ESO is as

$$\begin{aligned}\dot{\hat{x}}_{11} &= \hat{x}_{21} + \beta_1[x_{11} - \hat{x}_{11}] \\ \dot{\hat{x}}_{12} &= \hat{x}_{22} + \beta_1[x_{12} - \hat{x}_{12}] \\ \dot{\hat{x}}_{21} &= \hat{x}_{31} + \beta_2[x_{11} - \hat{x}_{11}] \\ \dot{\hat{x}}_{22} &= \hat{x}_{32} + \beta_2[x_{12} - \hat{x}_{12}] + u_2 \\ \dot{\hat{x}}_{31} &= \beta_3[x_{11} - \hat{x}_{11}] \\ \dot{\hat{x}}_{32} &= \beta_3[x_{12} - \hat{x}_{12}]\end{aligned}\tag{4.2}$$

Where, the time-varying gain factors  $\{\beta_i\}_{i=1}^3$  are proposed as (3.3)–(3.6).

$$\beta_i = L_i + \bar{\beta}_{i,1} \frac{2+i}{T} (1 - \mu_1^{-1}) \mu_1^{i-1} - \bar{\beta}_{i+1,1} \mu_1^i - \sum_{j=1}^{i-1} \bar{\beta}_{i,j} \mu_1^{i-j} \beta_j, i = 1, 2\tag{4.3}$$

$$\beta_3 = L_3 + \bar{\beta}_{3,1} \frac{5}{T} (1 - \mu_1^{-1}) \mu_1^2 - \sum_{j=1}^2 \bar{\beta}_{3,j} \mu_1^{3-j} \beta_j\tag{4.4}$$

Where,  $\{\bar{\beta}_{2,j}\}$  for  $j = 2, 3$  are expressed as follows:

$$\bar{\beta}_{2,j-1} = \bar{\beta}_{2,j} \frac{\mu_1^{-1}}{T} (5 + \mu_1^{-1} - j(1 + \mu_1^{-1})) + \bar{\beta}_{3,j}\tag{4.5}$$

$$\bar{\beta}_{3,j-1} = \bar{\beta}_{3,j} \frac{\mu_1^{-1}}{T/3} \left(2 - \frac{j}{T} (1 - \mu_1^{-1})\right), i = 3\tag{4.6}$$

Its structure only relies on selecting the gains  $\{L_i\}$  to induce the matrix  $A = \begin{bmatrix} -L_1 & 1 & 0 \\ -L_2 & 0 & 1 \\ -L_3 & 0 & 0 \end{bmatrix}$

Hurwitz, afterwards selecting the designed parameter  $T$  independently to regulate the convergence time.

The results of the simulation are displayed in Figures 2–8. In Figure 2, it is seen that the state  $q_1$  follows the reference input  $q_{r1}$ , the estimated state  $\hat{q}_1$  follows  $q_1$  and it exhibits the system state  $q_2$ , the reference signal  $q_{r2}$  and the estimated state  $\hat{q}_2$ . Figure 3 indicates that the error  $e_{11}$  for  $q_1 - q_{r1}$  is bounded, the error  $e_{12}$  for  $\hat{q}_1 - q_1$  is bounded. Similarly, Figure 4 exhibits that the error  $e_{21}$  for  $q_2 - q_{r2}$  is bounded, and the error  $e_{22}$  for  $\hat{q}_2 - q_2$  is bounded. Figure 5 indicates that the estimated state  $d\hat{q}_1$  follows the system state differential  $dq_1$ , the estimated state  $d\hat{q}_2$  follows the system state differential  $dq_2$ . Figure 6 indicates the applied control input signal  $u_1$  and  $u_2$ . Figure 7 illustrates that the trajectories of adaptive rate  $\|\theta\|_2$ . In order to compare the difference between the finite-time application results and the infinite-time application results, we carried out a comparative simulation. The premise is to adjust best, the parameters of the two controllers by the trial-and-error method. Figure 8 illustrates that the finite-time methods show better error convergence performance.

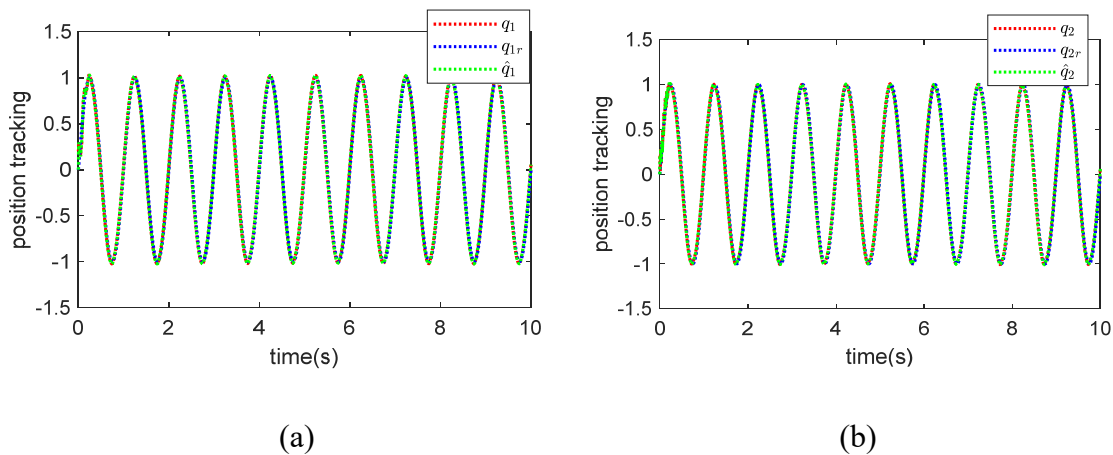


**Figure 2.** The trajectories of  $q_1$ ,  $q_{r1}$ ,  $\hat{q}_1$  and  $q_2$ ,  $q_{r2}$ ,  $\hat{q}_2$ .

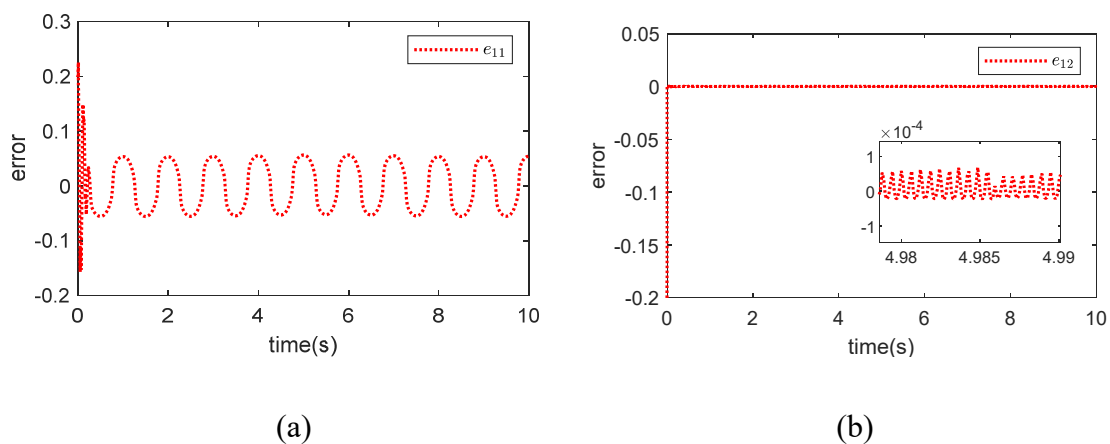


**Figure 3.** The trajectory of tracking errors  $e_{11}$ ,  $e_{12}$ .

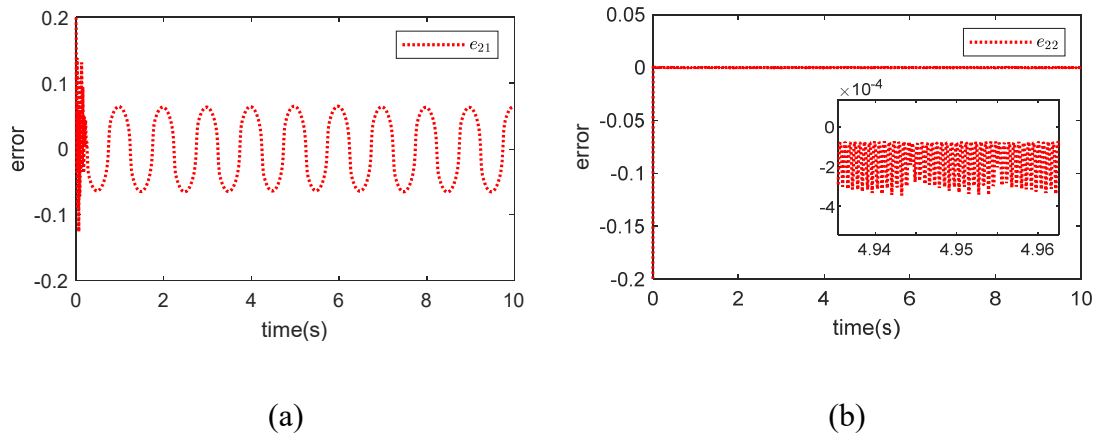


**Figure 4.** The trajectory of tracking errors  $e_{21}$ ,  $e_{22}$ .

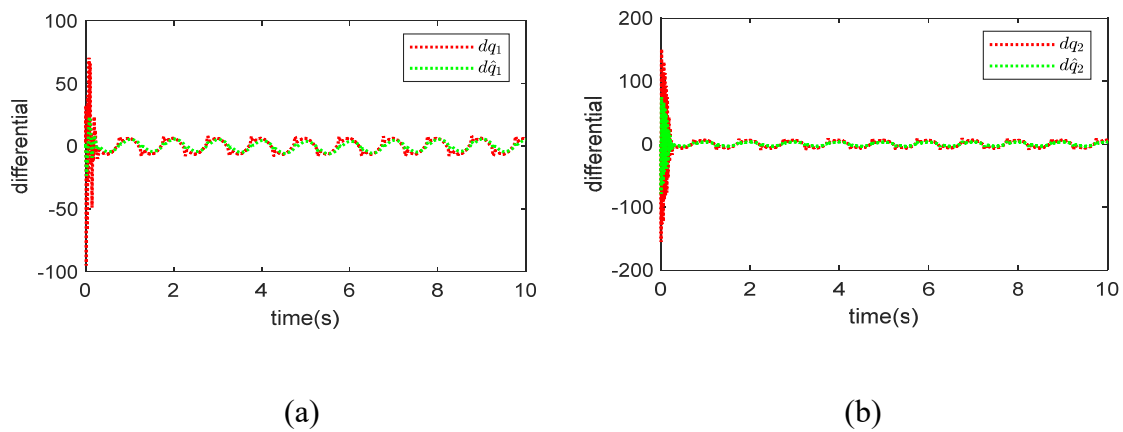


**Figure 5.** The trajectories of  $dq_1$ ,  $d\hat{q}_1$  and  $dq_2$ ,  $d\hat{q}_2$ .

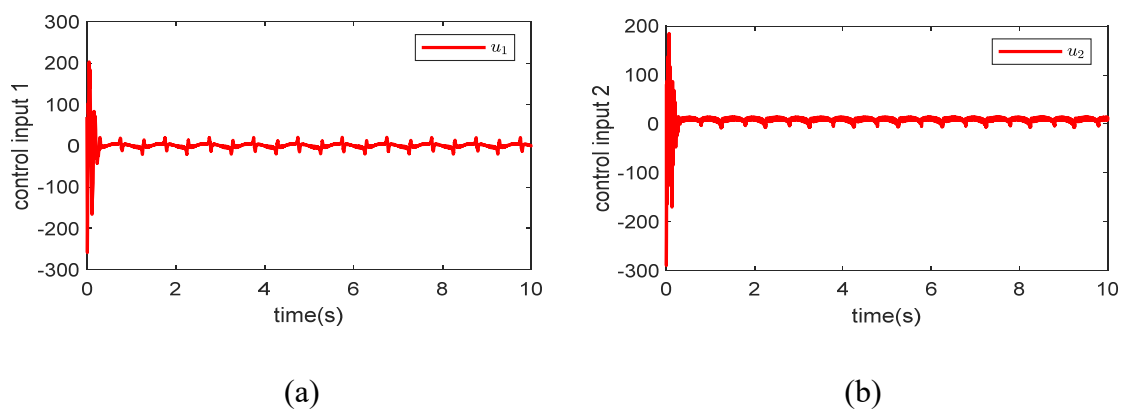


**Figure 6.** The trajectories of control input  $u_1$ ,  $u_2$ .

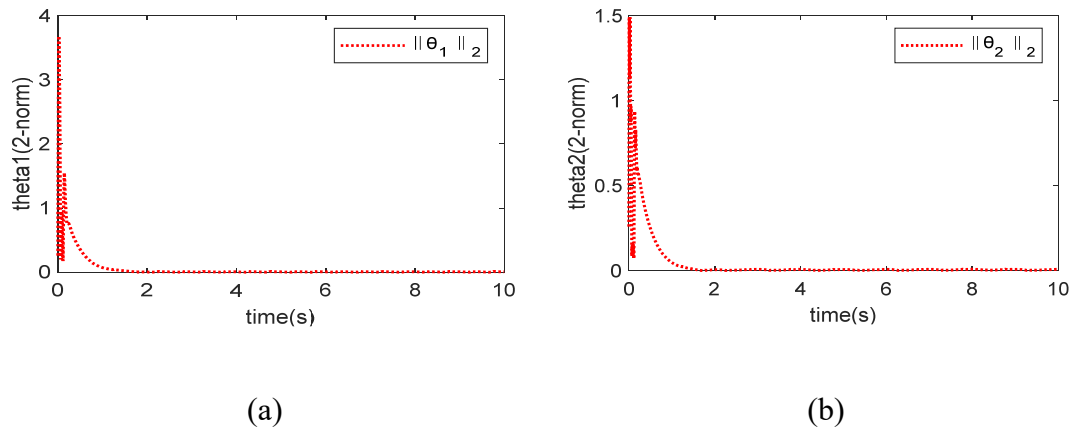


**Figure 7.** The trajectory of  $\|\theta_1\|_2$ ,  $\|\theta_2\|_2$ .

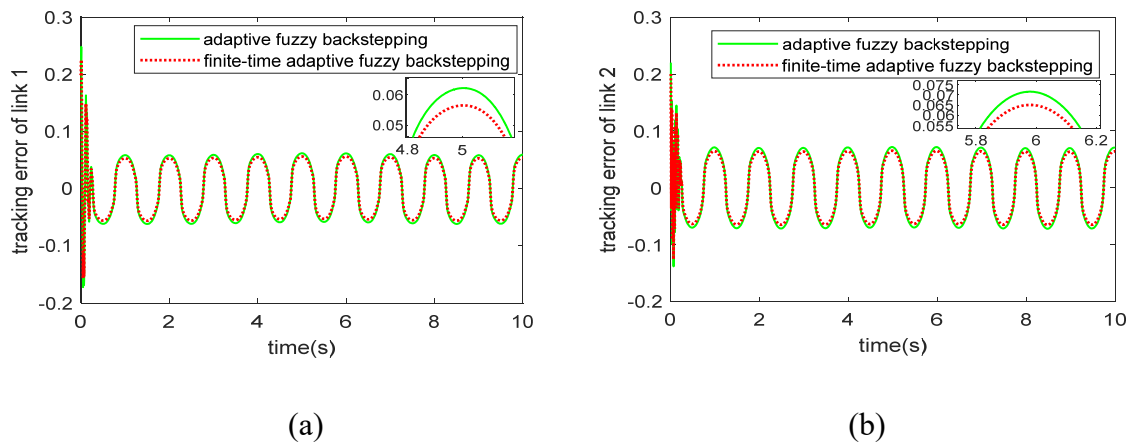


**Figure 8.** Tracking errors of link 1 and link 2.

The results of the simulation clearly show that the finite-time fuzzy adaptive back-stepping control strategy based on FT-ESO can guarantee that all the state variables of the system are SGPFS, and the tracking error gets into a tiny neighborhood around the origin in a finite time.

## 5. Conclusions

This research proposed a fuzzy adaptive control method for a class of MIMO coupled nonlinear systems by combining the back-stepping technique, finite time theory and FT-ESO. The back-stepping technique is used by transforming the general form of the coupled nonlinear system. Then the virtual control input is introduced and the fuzzy adaptive control rate is designed for the new form of the system according to the back-stepping technique. The fuzzy approximation function is included in the actual control signal. Furthermore, due to the introduction of FT-ESO, the proposed control approach does not need the states of the control systems to be directly measured. The finite-time Lyapunov function can ensure the closed-loop systems stability. This method solves the problem of application of fuzzy adaptive control, which is difficult to apply to a class of coupled nonlinear systems with immeasurable states and uncertainties. The efficacy of the proposed strategy is verified by the

simulations. Considering some practical situations, future research will focus on systems with the input saturations or dead zones.

## Acknowledgments

This work is financially sponsored by the Liaoning Provincial Department of Education General Projects (LJKR0677, LJKR0716).

## Conflict of interest

The authors declare that they have no conflicts of interest to report regarding the present study.

## References

1. F. Lin, P. Shieh, P. Chou, Robust Adaptive back-stepping motion control of linear ultrasonic motors using fuzzy neural network, *IEEE Trans. Fuzzy Syst.*, **16** (2008), 676–692. <https://doi.org/10.1109/TFUZZ.2008.921400>
2. C. Lin, H. Li, TSK Fuzzy CMAC-based robust adaptive back-stepping control for uncertain nonlinear systems, *IEEE Trans. Fuzzy Syst.*, **20** (2012), 1147–1154. <https://doi.org/10.1109/TFUZZ.2012.2191789>
3. J. Peng, R. Dubay, Adaptive fuzzy back-stepping control for a class of uncertain nonlinear strict-feedback systems based on dynamic surface control approach, *Expert Syst. Appl.*, **120** (2019), 239–252. <https://doi.org/10.1016/j.eswa.2018.11.040>
4. W. Min, Q. Liu, An improved adaptive fuzzy back-stepping control for nonlinear mechanical systems with mismatched uncertainties, *Automatika*, **60** (2019), 1–10. <https://doi.org/10.1080/00051144.2018.1563357>
5. C. Lin, C. Hsueh, C. Chen, Robust adaptive back-stepping control for a class of nonlinear systems using recurrent wavelet neural network, *Neurocomputing*, **142** (2014), 372–382. <https://doi.org/10.1016/j.neucom.2014.04.023>
6. X. Cao, P. Shi, Z. Li, M. Liu, Neural-network-based adaptive back-stepping control with application to spacecraft attitude regulation, *IEEE Trans. Neural Networks Learn. Syst.*, **29** (2018), 4303–4313. <https://doi.org/10.1109/TNNLS.2017.2756993>
7. W. Chen, L. Jiao, R. Li, J. Li, Adaptive back-stepping fuzzy control for nonlinearly parameterized systems with periodic disturbances, *IEEE Trans. Fuzzy Syst.*, **18** (2010), 674–685. <https://doi.org/10.1109/TFUZZ.2010.2046329>
8. Y. Liu, Q. Zhu, N. Zhao, L. Wang, Adaptive fuzzy back-stepping control for nonstrict feedback nonlinear systems with time-varying state constraints and backlash-like hysteresis, *Inf. Sci.*, **574** (2021), 606–624. <https://doi.org/10.1016/j.ins.2021.07.068>
9. X. Y. Luo, Z. H. Zhu, X. P. Guan, Adaptive fuzzy dynamic surface control for uncertain nonlinear systems, *Int. J. Autom. Comput.*, **6** (2009), 385–390. <https://doi.org/10.1007/s11633-009-0385-z>
10. P. Chen, T. Zhang, Adaptive dynamic surface control of stochastic nonstrict feedback constrained nonlinear systems with input and state unmodeled dynamics, *Int. J. Adapt. Control Signal Process.*, **34** (2020), 1405–1429. <https://doi.org/10.1002/acs.3157>



11. J. Yu, Y. Ma, H. Yu, C. Lin, Adaptive fuzzy dynamic surface control for induction motors with iron losses in electric vehicle drive systems via back-stepping, *Inf. Sci.*, **376** (2017), 172–189. <https://doi.org/10.1016/j.ins.2016.10.018>
12. Q. Zhao, Y. Lin, Adaptive fuzzy dynamic surface control with pre-specified tracking performance for a class of nonlinear systems, *Asian J. Control*, **13** (2011), 1082–1091. <https://doi.org/10.1002/asjc.236>
13. X. Shi, Y. Cheng, C. Yin, X. Huang, S. Zhong, Design of adaptive back-stepping dynamic with RBF neural network for uncertain nonlinear system surface control method, *Neurocomputing*, **330** (2019), 490–503. <https://doi.org/10.1016/j.neucom.2018.11.029>
14. H. Dastres, B. Rezaie, B. Baigzadehnoe, Neural-network-based adaptive back-stepping control for a class of unknown nonlinear time-delay systems with unknown input saturation, *Neurocomputing*, **398** (2020), 131–152. <https://doi.org/10.1016/j.neucom.2020.02.070>
15. S. Tong, C. Li, Y. Li, Fuzzy adaptive observer back-stepping control for MIMO nonlinear systems, *Fuzzy Sets Syst.*, **160** (2009), 2755–2775. <https://doi.org/10.1016/j.fss.2009.03.008>
16. C. Lee, J. Chien, H. Chang, C. Kuo, H. Chang, Direct adaptive back-stepping control for a class of mimo non-affine systems using recurrent neural networks, *Lect. Notes Eng. Comput. Sci.*, (2009), 2174.
17. S. C. Tong, Y. M. Li, G. Feng, T. S. Li, Observer-based adaptive fuzzy back-stepping dynamic surface control for a class of MIMO nonlinear systems, *IEEE Trans. Syst. Man Cybern. Part B Cybern.*, **41** (2011), 1124–1135. <https://doi.org/10.1109/TSMCB.2011.2108283>
18. W. Chen, J. Li, Globally decentralized adaptive back-stepping neural network tracking control for unknown nonlinear interconnected systems, *Asian J. Control*, **12** (2010), 96–102. <https://doi.org/10.1002/asjc.160>
19. Y. Li, S. Tong, Y. Li, Observer-based adaptive fuzzy back-stepping dynamic surface control design and stability analysis for MIMO stochastic nonlinear systems, *Nonlinear Dyn.*, **69** (2012), 1333–1349. <https://doi.org/10.1007/s11071-012-0351-0>
20. Y. Liu, Q. Zhu, Adaptive neural network asymptotic control design for MIMO nonlinear systems based on event-triggered mechanism, *Inf. Sci.*, **603** (2022), 91–105. <https://doi.org/10.1016/j.ins.2022.04.048>
21. K. Zheng, Q. Zhang, Y. Hu, B. Wu, Design of fuzzy system-fuzzy neural network back-stepping control for complex robot system, *Inf. Sci.*, **546** (2021), 1230–1255. <https://doi.org/10.1016/j.ins.2020.08.110>
22. F. Lin, P. Chou, Adaptive control of two-axis motion control system using interval type-2 fuzzy neural network, *IEEE Trans. Ind. Electron.*, **56** (2009), 178–193. <https://doi.org/10.1109/TIE.2008.927225>
23. J. Huang, M. Ri, D. Wu, S. Ri, Interval type-2 fuzzy logic modeling and control of a mobile two-wheeled inverted pendulum, *IEEE Trans. Fuzzy Syst.*, **26** (2018), 2030–2038. <https://doi.org/10.1109/TFUZZ.2017.2760283>
24. M. Y. Hsiao, T. H. S. Li, J. Z. Lee, C. H. Chao, S. H. Tsai, Design of interval type-2 fuzzy sliding-mode controller, *Inf. Sci.*, **178** (2008), 1696–1716. <https://doi.org/10.1016/j.ins.2007.10.019>
25. R. Shahnazi, Observer-based adaptive interval type-2 fuzzy control of uncertain MIMO nonlinear systems with unknown asymmetric saturation actuators, *Neurocomputing*, **171** (2016), 1053–1065. <https://doi.org/10.1016/j.neucom.2015.07.098>

26. Y. Chang, W. Chan, Adaptive dynamic surface control for uncertain nonlinear systems with interval type-2 fuzzy neural networks, *IEEE Trans. Cybern.*, **44** (2014), 293–304. <https://doi.org/10.1109/TCYB.2013.2253548>
27. S. Dian, Y. Hu, T. Zhao, J. Han, Adaptive back-stepping control for flexible-joint manipulator using interval type-2 fuzzy neural network approximator, *Nonlinear Dyn.*, **97** (2019), 1567–1580. <https://doi.org/10.1007/s11071-019-05073-8>
28. R. Rahmani, H. Toshani, S. Mobayen, Consensus tracking of multi-agent systems using constrained neural-optimiser-based sliding mode control, *Int. J. Syst. Sci.*, **51** (2020), 2653–2674. <https://doi.org/10.1080/00207721.2020.1799257>
29. W. Liu, Q. Ma, S. Xu, Z. Zhang, Adaptive finite-time event-triggered control for nonlinear systems with quantized input signals, *Int. J. Robust Nonlinear Control*, **31** (2021), 4764–4781. <https://doi.org/10.1002/rnc.5510>
30. J. Ding, W. Zhang, Finite-time adaptive control for nonlinear systems with uncertain parameters based on the command filters, *Int. J. Robust Nonlinear Control*, **35** (2021), 1754–1767. <https://doi.org/10.1002/acs.3287>
31. S. Xie, M. Tao, Q. Chen, L. Tao, Neural-network-based adaptive finite-time output constraint control for rigid spacecrafts, *Int. J. Robust Nonlinear Control*, **32** (2022), 2983–3000. <https://doi.org/10.1002/rnc.5766>
32. Y. Wu, X. Xie, Adaptive pre-assigned finite-time stability of nonlinear systems with time-varying powers and full-state constraints, *Int. J. Robust Nonlinear Control*, **32** (2022), 2200–2211. <https://doi.org/10.1002/rnc.5940>
33. H. Liu, T. Zhang, Adaptive neural network finite-time control for uncertain robotic manipulators, *J. Intell. Rob. Syst.*, **75** (2014), 363–377. <https://doi.org/10.1007/s10846-013-9888-5>
34. C. W. Chang, C. F. Hsu, T. T. Lee, Back-stepping-based finite-time adaptive fuzzy control of unknown nonlinear systems, *Int. J. Fuzzy Syst.*, **20** (2018), 2545–2555. <https://doi.org/10.1007/s40815-018-0505-4>
35. Y. Li, K. Li, S. Tong, Finite-time adaptive fuzzy output feedback dynamic surface control for MIMO non-strict feedback systems, *IEEE Trans. Fuzzy Syst.*, **27** (2019), 96–110. <https://doi.org/10.1109/TFUZZ.2018.2868898>
36. S. Sui, C. L. P. Chen, S. Tong, Event-trigger-based finite-time fuzzy adaptive control for stochastic nonlinear system with unmodeled dynamics, *IEEE Trans. Fuzzy Syst.*, **29** (2021), 1914–1926. <https://doi.org/10.1109/TFUZZ.2020.2988849>
37. H. Wang, S. Kang, Z. Feng, Finite-time adaptive fuzzy command filtered backstepping control for a class of nonlinear systems, *Int. J. Fuzzy Syst.*, **21** (2019), 2575–2587. <https://doi.org/10.1007/s40815-019-00749-0>
38. L. Liu, W. Zhao, Y. J. Liu, S. Tong, Y. Y. Wang, Adaptive finite-time neural network control of nonlinear systems with multiple objective constraints and application to electromechanical system, *IEEE Trans. Neural Networks Learn. Syst.*, **32** (2021), 5416–5426. <https://doi.org/10.1109/TNNLS.2020.3027689>
39. L. Liu, Y. Cui, Y. J. Liu, S. Tong, Observer-based adaptive neural output feedback constraint controller design for switched systems under average dwell time, *IEEE Trans. Circuits Syst. I Regul. Pap.*, **68** (2021), 3901–3912. <https://doi.org/10.1109/TCSI.2021.3093326>

40. F. Wang, B. Chen, C. Lin, J. Zhang, X. Z. Meng, Adaptive neural network finite-time output feedback control of quantized nonlinear systems, *IEEE Trans. Cybern.*, **48** (2018), 1839–1848. <https://doi.org/10.1109/TCYB.2017.2715980>
41. B. Chen, F. Wang, X. P. Liu, C. Lin, Finite-time adaptive fuzzy tracking control design for nonlinear systems, *IEEE Trans. Fuzzy Syst.*, **26** (2018), 1209–1216. <https://doi.org/10.1109/TFUZZ.2017.2717804>
42. H. Razmjooei, M. H. Shafiei, A new approach to design a finite-time extended state observer: uncertain robotic manipulators application, *Int. J. Robust Nonlinear Control*, **31** (2021), 1288–1302. <https://doi.org/10.1002/rnc.5346>



AIMS Press

©2022 the Author(s), licensee AIMS Press. This is an open access article distributed under the terms of the Creative Commons Attribution License (<http://creativecommons.org/licenses/by/4.0>)